The lack of paleosol features and the presence of small body fossils indicates a different origin for the blocky mudstones of the Island Creek. The blocky mudstones of the Island Creek are interpreted as prodelta deposits. Prodelta deposits are characteristically fine-grained muddy sediments often containing shell remains and plant and wood debris (Reineck & Singh, 1975). Shepard (1957) described prodeltaic deposits of the modern Mississippi as homogeneous, structureless fine-grained clays and silty clays deposited in water depths greater than about 120 feet.

Stratigraphic Correlations and Sequence-Stratigraphic Interpretations

The stratigraphic correlations discussed below are illustrated in Figures 2.30 to 2.34. These figures are cross-sections and a fence diagram that present information gathered from stratigraphic description of outcrops, quarry exposures, and drill cores. Detailed measured stratigraphic sections of all localities are in Appendix 1. The goal of these correlations is to establish a sequence-stratigraphic framework that identifies sequence boundaries that indicate rise and fall of sea level as well as other significant stratigraphic surfaces on a regional scale (e.g., flooding surfaces). The establishment of such a framework in which sea-level history is known allows the examination of other influences on deposition such as depositional topography and distribution of siliciclastics. The following sections present the regional and stratigraphic distribution of lithofacies and uses their interpreted depositonal environments and further detailed observations relevant to their sequence-stratigraphic interpretation to evaluate the controls on regional distribution of lithofacies.

Stratigraphic Datum

The basal bed of the upper Farley (30 to 90 cm thick) contains the only *Osagia*-brachiopod packstone facies found. This bed has consistent lithologic character and

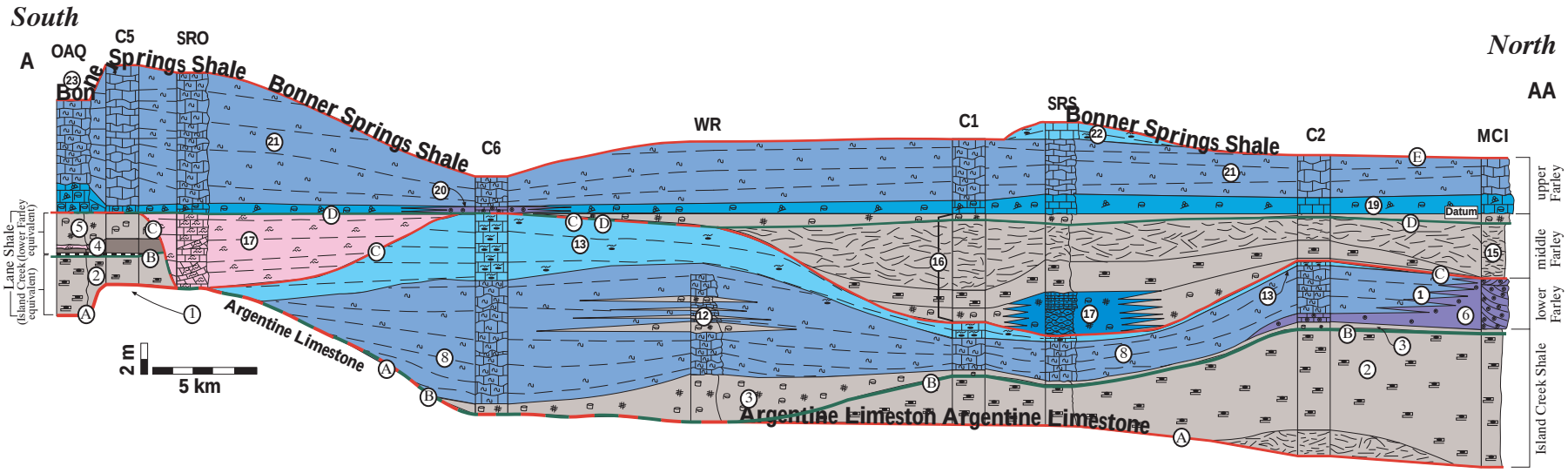

Figure 2.30. Reconstructed cross-section along line A-AA. Index map shows localities used all stratigraphic reconstructions. Legend outlines lithologic symbols and color codes used for this figure and Figures 2.31-2.33.

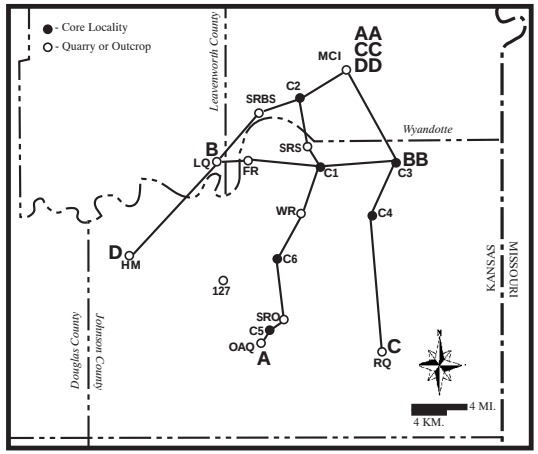

- Phylloid Algal Facies
- Skeletal Wackestone
- Peloidal, Skeletal Packstone
- *Osagia*, Brachiopod Wackestone
- Oolite
- Sandy, Skeletal Grainstone-Packstone
- Coal
- Dark, Organic-rich Mudstone
- Fossiliferous Siltstone
- Lenticular, Laminated Siltstone
- Blocky Mudstone
- # Feature Number/ Surface Letter
- Sequence Boundary
- Marine Flooding Surface
- Coincident Flooding Surface & Sequence Boundary

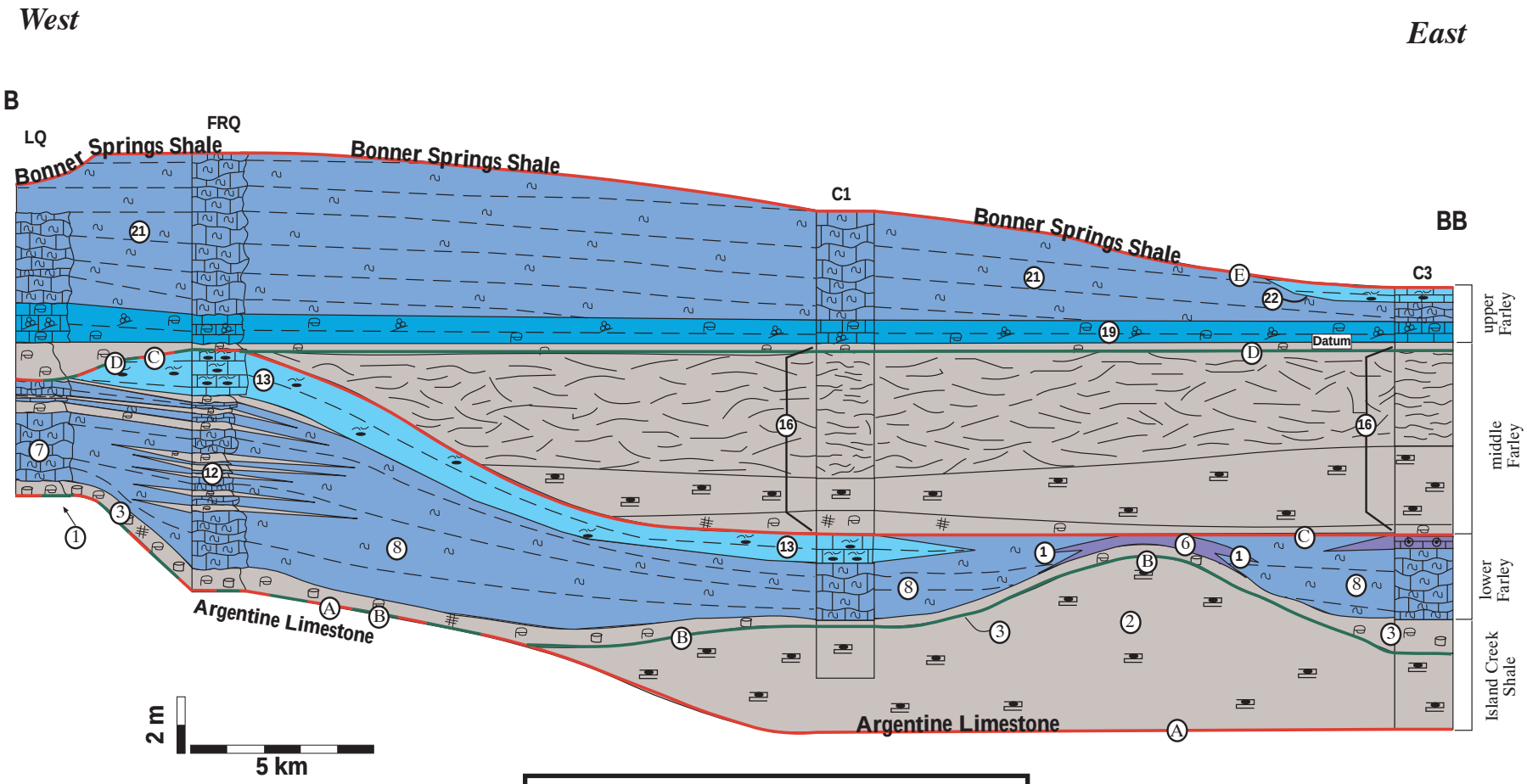

Figure 2.31. Reconstructed cross-sections along line B-BB. See figure 2.30 for legend and index map.

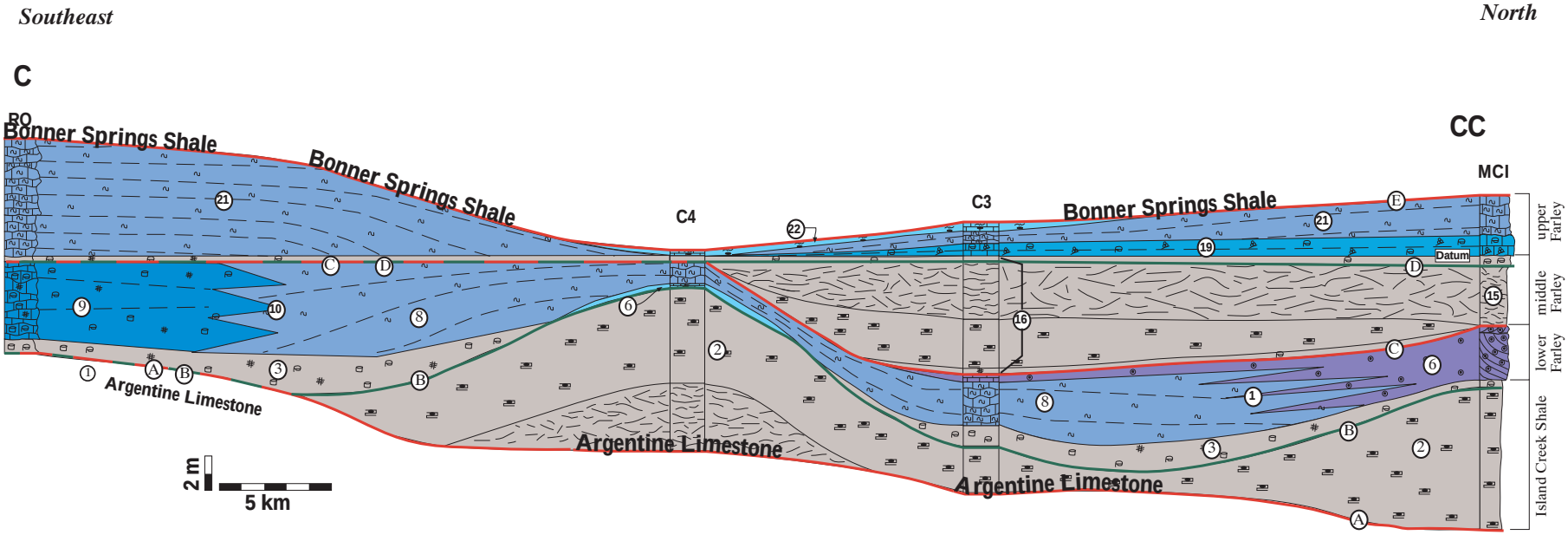

Figure 2.32. Reconstructed cross-sections along line C-CC. See Figure 2.30 for index map and legend.

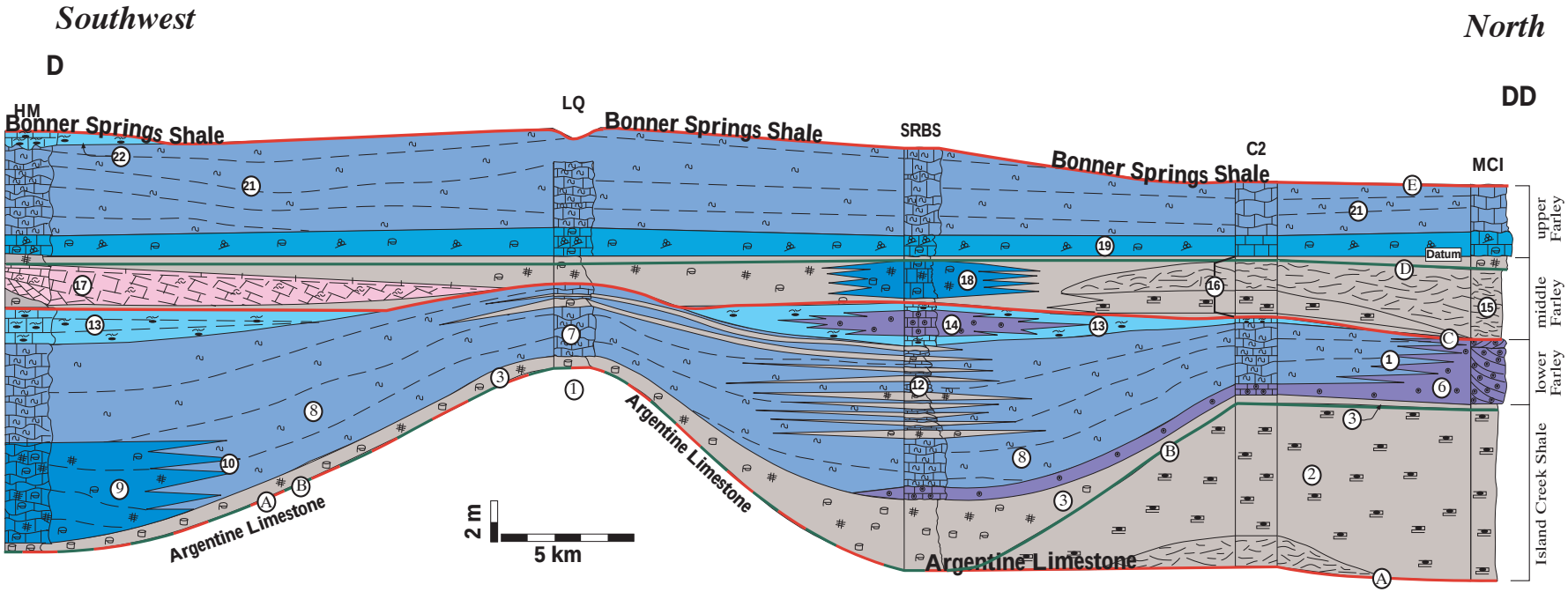

Figure 2.33. Reconstructed cross-section along line D-DD. See Figure 2.30 for locality map and legend.

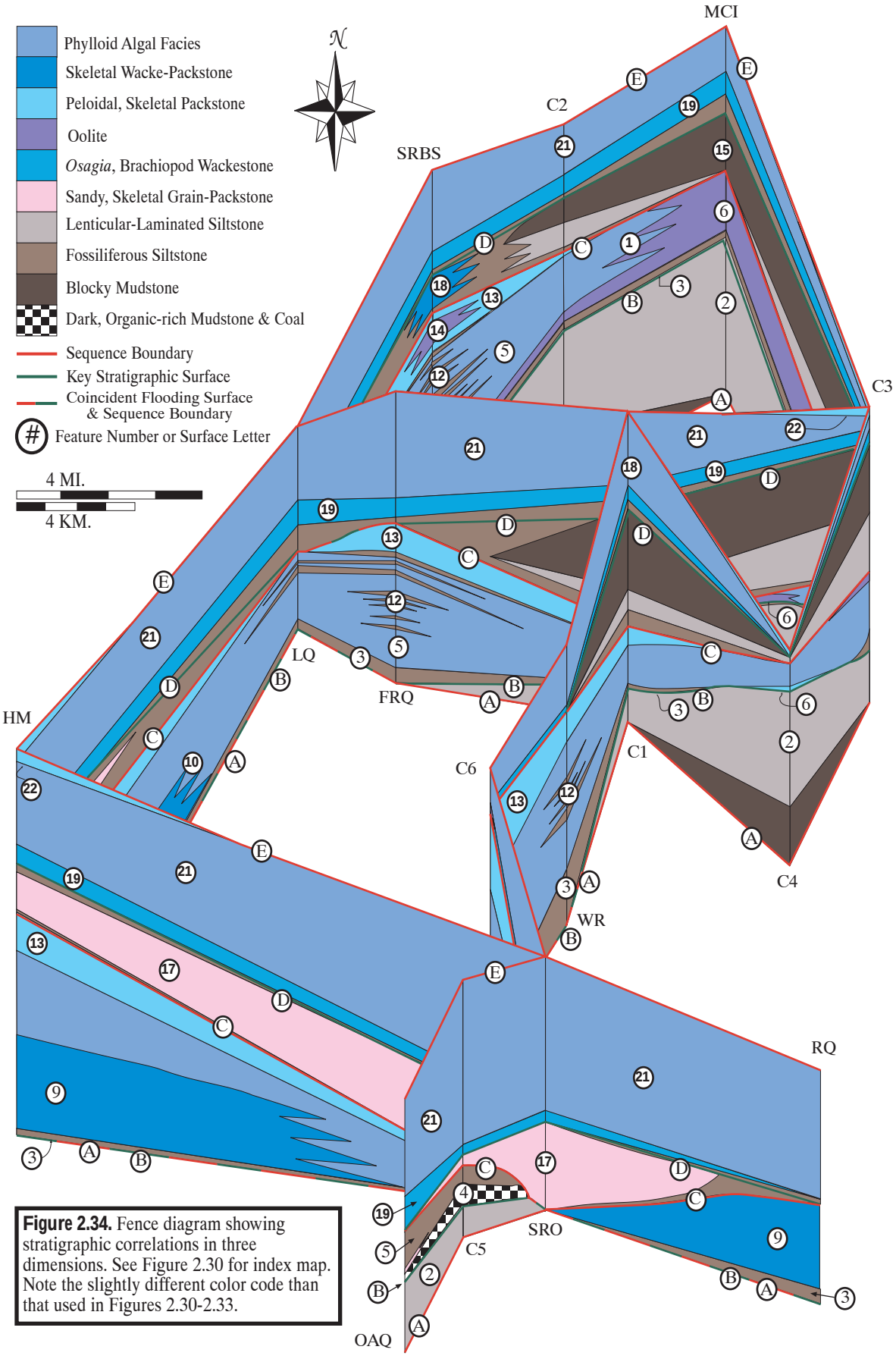

Figure 2.34. Fence diagram showing stratigraphic correlations in three dimensions. See Figure 2.30 for index map. Note the slightly different color code than that used in Figures 2.30-2.33.

stratigraphic location throughout the field area. The bed is recognized by a zone of whole brachiopods, brachiopod fragments, and other skeletal fragments that are encrusted with *Osagia*. The lithologic consistency of this thin bed suggests a similar environment throughout the area and is interpreted to have been deposited on a relatively flat depositional surface. For these reasons, the basal bed of the upper Farley makes an excellent marker bed and is the datum for the stratigraphic reconstructions (Figures 2.30 to 2.33). Use of this datum allows the closest possible reconstruction of actual depositional topography.

Isopach mapping based on data from Crowley (1969) and this study (Fig. 2.3) shows thickened areas of Argentine Limestone in the northeast, northwest, and southeast corners with an additional, slightly thickened area near the center of the field area. These topographic highs in the Argentine are also apparent in the reconstructed cross-sections (Figs. 2.30-2.33: Feature 1), which further indicates that the basal bed of the upper Farley is a reasonable datum to use for the stratigraphic reconstructions.

The stratigraphic reconstructions offered do not depict exact depositional topography for two main reasons. First, other regional work by Watney *et al.* (1989) suggests that the area may have had a slight south-southwestward dip that cannot be shown in the cross-sections. Second, compaction of shale and silt following deposition can alter thicknesses of a stratigraphic succession by as much as 40-50 percent (Tucker, 1991). These factors provide additional difficulties when attempting to accurately depict depositional topography. The following discussion separates the correlated strata into three stratigraphic intervals with related surfaces and discusses their origin.

Argentine Limestone (Stratigraphic Surface A)

The Argentine Limestone is the carbonate unit located directly under the Lane-Island Creek shales or the Farley Limestone at all localities (Figures 2.30-2.33). The

Argentine Limestone has been interpreted as a fully marine unit with such facies as phylloid algal packstones, oolite, and skeletal packstone (Crowley, 1969; Watney *et al.*, 1989; Arvidson, 1990; this study)

Throughout the field area the Argentine Limestone has an irregular surface near its top that has been interpreted as a marine hardground or firmground (Watney *et al.*, 1989). This surface is most prominently developed in the west, center, and south (Localities HM, RQ, WR) where it is overlain by a thin fossiliferous siltstone. These areas received little to no siliciclastic influx, and this surface near the top of the Argentine represents the first significant surface in the sequence-stratigraphic framework of the Lane-Island Creek shales and the Farley Limestone (Figures 2.30-2.34: Surface A). This surface appears to be a surface of nondeposition that coincides with the time period between termination of Argentine carbonate deposition and the influx of the siliciclastics of the Lane-Island Creek shales discussed below.

Lane-Island Creek Interval

Directly overlying the Argentine Limestone in the north (localities MCI, C2), east (locality C4), and the south (localities OAQ, C5) are thick siltstones that are somewhat thinner in the east and west-central areas (localities SRS, C1 & C3) (Figures 2.30-2.34: Feature 2). These siltstones comprise the Lane-Island Creek shales, and the facies present are dominantly laminated to lenticular bedded siltstones but also include local accumulations of blocky mudstone. As discussed previously, these siltstone facies are interpreted as delta front to prodelta deposits. It is important to consider what controlled the distribution of these deposits.

Isopach mapping of the Lane-Island Creek interval (Fig. 2.4) suggests that the siliciclastics form two separate deltaic units with source in different directions. The Island Creek appears to have a northern source, whereas the Lane has a southern source.

Comparison of isopach maps for the Argentine Limestone and the Lane-Island Creek shales (Figs 2.3 & 2.4) suggest that the distribution of the deltaic siliciclastics was closely controlled by the subtle depositional topography of the Argentine Limestone. There are paleotopographic highs (thicks) in the Argentine Limestone in the northwest and northeast corners of the field area, and the Island Creek appears to fill a channel-shaped depositional low between these two topographic highs. Furthermore, the Island Creek delta thins into and terminates against a topographic high in the Argentine in the southeast corner of the area (Figures 2.3 & 2.4). This distribution of siliciclastics suggests that the deltaic deposits of the Island Creek did not form a topographically positive lobe or wedge as suggested by earlier authors (Crowley, 1969; Arvidson, 1990). Instead, these deltaic siliciclastics seemed to have behaved more as valley fills by filling depositonal lows in the underlying limestone.

Distribution of the Lane deltaic sediments in the southern part of the field area also appears to have been controlled by the paleotopography of the Argentine Limestone (Figures 2.3 & 2.4). The lower part of the Lane delta extends into the area from the southwest and covers a broad area. This broad distribution could have been because there were fewer topographic restrictions on the underlying Argentine Limestone (Figure 2.4). The same isopach maps (Figs. 2.3 & 2.4) suggest that the siliciclastics of the Lane-Island Creek deltas in part onlapped highs in the Argentine Limestone.

The presence of deltaic siliciclastics immediately overlying the marine Argentine Limestone is interpreted as the result of a relative fall in sea level. This relative sea-level fall allowed the influx of deltaic siliciclastics from the north (Island Creek) and the south (Lane), which terminated deposition of Argentine carbonates. Interpretation of a relative sea-level fall is supported by the presence of two separate deltaic units that encroached into the area from different directions at the same time. Although the presence of deltaic sediments overlying Argentine carbonates could have resulted from autogenic delta-lobe

switching, the presence of two deltas entering the area from different directions at the same time would be unexpected; their migration is more likely the result of a relative sea-level fall. Thus, the boundary separating the underlying Argentine Limestone from the overlying siliciclastics of the Lane-Island Creek shales is interpreted as a sequence boundary (Figures 2.30 to 2.34: Surface A).

A lack of evidence of subaerial exposure in the Lane-Island Creek or along the top of the Argentine Limestone indicates that the relative sea-level fall was not extensive enough to expose the upper surface of the Argentine within the study area. It was, however, great enough to allow deltas to enter the area from both the north and south. This increase in siliciclastic input effectively shut down carbonate production. In areas receiving no deltaic siliciclastic influx, a marine hardground developed in the upper portion of the Argentine Limestone.

Upper Island Creek-Lower Farley Interval

The lower Farley interval consists of a variety of siltstone and carbonate facies throughout the field area. The initial deposits of this interval are fossiliferous siltstones that are interpreted as accumulations of marine, prodeltaic sediments. These deposits overlie the deltaic siliciclastics of the Island Creek in the north and occur immediately over the Argentine Limestone in the western, southwestern, and central portions of the area where there are no deltaic siliciclastics (Figures 2.30 to 2.34: Feature 3). The fossiliferous siltstones are not present over the deltaic siliciclastics to the south in the area of the Lane delta. Instead, in this area the deposits immediately overlying the deltaic siliciclastics are composed of coal and dark, organic-rich shale with a local accumulation of sandy, skeletal grainstone-packstone (Figures 2.30, 2.34: Feature 4).

The fossiliferous siltstones to the north and west are correlated with the coal and dark, organic-rich mudstones and sandy, skeletal grainstone-packstones in the middle portion of the Lane delta to the south because the fossiliferous siltstones and the coal and dark, organic-rich mudstones and grainy skeletal bed all provide evidence of a marine flooding unit. These lithologies are similar to those described for flooding units in other similar Pennsylvanian units by Watney *et al.*, (1989), who stated that lithologies such as thin, fossiliferous siltstones as well as coals capped by invertebrate skeletal lags, are typically flooding units in Pennsylvanian depositional sequences. Furthermore, the widespread, regional extent of these marine lithologies suggests a major flooding event. Thus, the fossiliferous siltstones and the coal and dark, organic-rich mudstone capped by the sandy, skeletal grainstone-packstone are a single flooding unit expressed as different lithologies. Because flooding surfaces are important in interpreting the sequence stratigraphy, the base of this flooding unit is identified as the next key stratigraphic surface (Figures 2.30 to 2.34: Surface B).

Based on its lithofacies, the environments represented by the flooding unit have been interpreted as marine (fossiliferous siltstone) or restricted marine (dark, organic-rich mudstone). This switch to more marine facies suggests that siliciclastic sources had become more distal, and waters were more normal marine in salinity. Therefore, the transition from deltaic clastics to marine or restricted marine clastics probably resulted from a relative rise in sea level. In areas that received little to no deltaic influx, the marine flooding surface coincides with surface A, so that surfaces A and B are coincident in places.

Following the relative rise of sea level, carbonate production was established in all areas except the area of the Lane delta in the south, where fossiliferous siltstones continued to accumulate as prodelta deposits of the Lane delta while the lower Farley carbonates were being deposited (Figures 2.30, 2.34: Feature 5). Oolites and peloidal, skeletal packstones accumulated in the north and east along topographic highs formed by the thick

complex of the Island Creek siliciclastics (Figures 2.30 to 2.34: Feature 6). The thickness of the deltaic deposits produced a slight topographic prominence along which elevated energies prevailed due to shallower water depths. Phylloid algal facies are located in lows and directly over topographic highs (Figs. 2.31, 2.33: Feature 7) in the west, indicating deeper water depths to the west. Such an increase in depth was likely to have been due to original depositional slope which was approximately 0.6 $^{m}/_{km}$ to the west-southwest (Watney et al, 1989).

The greatest accumulations of phylloid-algal limestones in the lower Farley interval are generally located in topographic lows adjacent to topographic prominences on either the Argentine Limestone or the Island Creek delta. (Figures 2.30 to 2.33: Feature 8). Therefore, it appears most likely that the phylloid algae of the lower Farley Limestone did not contribute to the construction of depositional topography as suggested by previous authors (Heckel & Cocke, 1969; Harbaugh, 1959, 1960; Arvidson, 1990). Although interpretation of phylloid algae located in depositional lows is contrary to the normal interpretation of topography construction for such facies, it is not new. Matheny and Longman (1996) showed that some of the phylloid-algal facies of the Paradox Basin are concentrated in depositional lows caused by salt solution. Ball *et al.* (1977) suggested that phylloid algae did not construct topography but were instead only a source of sediment that typically collected in depositional lows between deltaic depocenters. The situation in the lower Farley Limestone is likely to have been a combination of these two interpretations. Much of the phylloid algal material is fragmental and apparently not in growth position, which suggests that it may have been transported into the depositional lows. There are, however, also occurrences of phylloid-algal boundstone that may have grown in the lows and not been transported. At this time the exact controls on the distribution of the phylloid algal facies are unknown.

In the southeast and southwest, in areas of deeper water farthest from deltaic siliciclastics, the quiet-water, skeletal wackestone-packstone facies was deposited (Figures 2.32 to 2.34: Feature 9). A more open-marine environment, promoted the deposition of the skeletal wackestone-packstone facies, was present in deeper, clear waters distal to the deltas and farther down the regional slope. Up the depositional slope to the north, there was a facies transition to phylloid-algal facies as water shallowed slightly (Figures 2.32 to 2.34: Feature 10). Farther to the north, the phylloid-algal facies grades to oolites where the shallowest water occurred (Figures 2.30, 2.31, 2.33, 2.34: Feature 11).

In one north-northwest to south-southeast trend, the lower Farley limestones are interbedded with marine shales and siliciclastics, becoming more abundant and coarser to the north-northwest (Figures 2.30-2.34: Feature 12). This suggests a shifted source of deltaic siliciclastics from the north-northwest with siliciclastics more abundant over underlying topographic lows. This supports the interpretation of Harris (1985) who suggested that the thin accumulations of siltstone in the Farley resulted from periodic influxes from the still active Island Creek delta to the northwest.

This shift in influx of siliciclastics is predictable given filling of the topography on the top of the Argentine Limestone by the Island Creek delta. The suggestion is that the siliciclastics in the lower Farley behaved in a manner similar to those of the Island Creek and preferentially filled depositional lows rather than constructing positive lobes or wedges. Because the valley in which the Island Creek siliciclastics were deposited was full or because sea-level rose above it, deposition of siliciclastics in the lower Farley shifted and found new low areas to fill.

In the western and central portions of the field area the lower Farley is capped by peloidal, skeletal packstone with local accumulations of oolitic, peloidal packstone (Figures

2.30, 2.31, 2.33, 2.34: Feature 13). These lithofacies indicate slightly elevated energy levels in which currents washed fine carbonate mud. An oolitic, peloidal packstone (locality SRBS) is sandwiched between beds of peloidal skeletal packstone (Figures 2.33, 2,34: Feature 14). This oolitic, peloidal packstone contains meniscus cement fabrics and keystone vugs, evidence for subaerial exposure of this facies prior to deposition of the immediately overlying peloidal, skeletal packstone.

The distribution of the peloidal, skeletal packstone facies is problematic. Peloidal, skeletal packstones and oolitic, peloidal packstones are located on and adjacent to topographic prominences in the lower Farley but not on the highest prominences. It is unknown what caused this distribution. One might have expected the highest energies to have been present on the paleotopographic highs and that packstones were generated there. But high energy present over the topographic highs may have swept carbonate sands off the highs into adjacent topographic depressions. Alternatively, currents may have been concentrated in paleotopographic low areas generating packstones in place.

The evidence of subaerial exposure within the deposits at locality SRBS suggests that deposition of the peloidal, skeletal packstones at the top of the lower Farley resulted from a relative fall in sea level. This would explain why the facies is present in the topographically lower areas and not found on the highest highs. If sea level fell, the topographic prominences may have been exposed subaerially and received no carbonate deposition. The presence of marine siltstone directly above these deposits, however, suggests that sea level may have risen again slightly following the deposition of the oolitic, peloidal packstone facies before continuing the drop that formed the sequence boundary located along the top of the lower Farley discussed below. This subtle fluctuation in sea level may help to explain the unusual distribution of peloidal, skeletal packstone facies within the lower Farley, with a minor relative sea-level fall bringing shallow waters and concentrating currents in paleotopographic lows.

Comparison of isopach maps for the lower Farley interval (Fig. 2.35) to those for the Argentine Limestone (Fig. 2.3) and the Lane-Island Creek shales (Fig. 2.4) illustrates that where the Argentine is thin the Lane-Island Creek is thick. Furthermore, where the lower Farley is thickest the Argentine Limestone is thin. Thus, the combined affect of Lane-Island Creek deposition followed by lower Farley Limestone deposition was to greatly reduce, but not completely eliminate, depositional topography. This is contrary to trends outlined by earlier authors (Heckel & Cocke, 1969; Crowley, 1969; Harbaugh, 1959, 1960; Arvidson, 1990) who suggested that thick accumulations of carbonates show a pronounced stacking pattern in which the thickest accumulations of one limestone directly overlie the thickest accumulations of the previous limestone unit thereby perpetuating topography upward in the stratigraphic section.

Top of Lower Farley-Middle Farley Interval

A prominent surface (Figs. 2.30-2.34: Surface C) separates the lower Farley from the middle Farley. Along this surface, nonmarine blocky mudstones with paleosols directly overlie marine limestones in the north (Figs. 2.30, 2.32-2.34: Feature 15) suggesting subaerial exposure and possible erosion. The presence of nonmarine, blocky mudstones immediately over lower Farley limestones indicates a sequence boundary between the two units (Figures 2.30-2.34: Surface C). Elsewhere, these blocky mudstones are underlain by fossiliferous siltstones and lenticular, laminated siltstones that sit atop the limestones of the lower Farley (Figures 2.30-2.33: Feature 16). Clearly, there must be some complex internal geometries within the siliciclastics of the middle Farley, the structure of which is as yet unknown. The

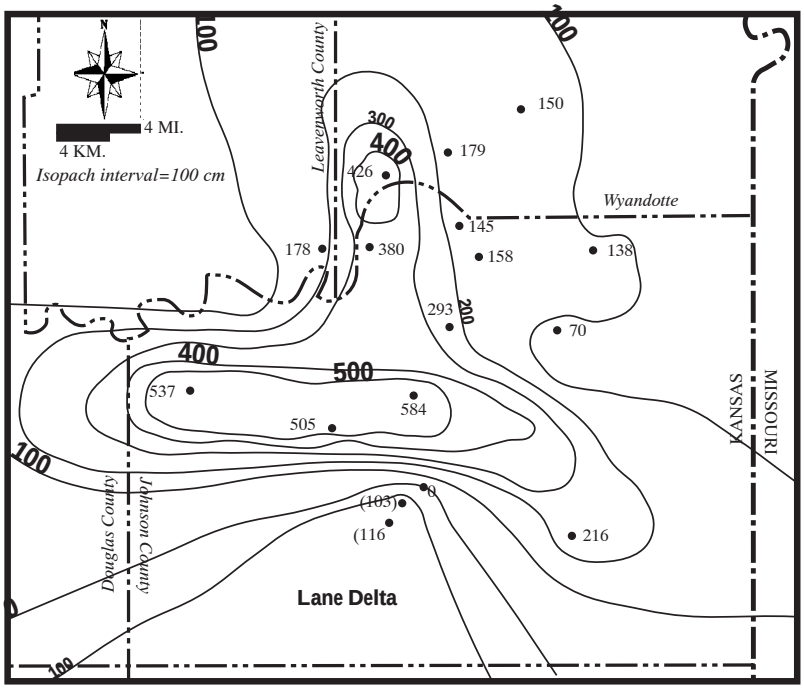

Figure 2.35. Isopach map of lower Farley limestone and equivalent shales to the south in the area of the Lane delta that was still active during deposition of the lower Farley. Note how the lower Farley thickness compliments the underlying Lane-Island Creek thickness variations illustrated in Figure 2.4. In areas where the Lane-Island Creek is thick, the lower Farley is thin and where the Lane-Island Creek shales are thin, the lower Farley is thick. The lower Farley limestone farther to the south is absent and instead is represented by a portion of the time-equivalent Lane Shale. Data from current study.

evidence for shallowing upward to nonmarine deposits in the middle Farley siliciclastics further supports the interpretation of a relative fall in sea level.

In addition to the siliciclastics discussed above, the middle Farley also contains deposits of sandy, skeletal grainstone and packstone (Figures 2.30, 2.33, 2.34: Feature 17). In the southwest, this facies is cross-bedded and located between beds of siliciclastics (Figures 2.33, 2.34: locality HM). This stratigraphic observation supports its correlation to other deposits of the middle Farley. In the south (localities SRO, C5), the sandy, skeletal grainstone-packstone is located in a trough-shaped low between the Lane delta to the south and a topographic high in the lower Farley to the north (Figures 2.30, 2.34-2.36).

This sandy, skeletal, cross-bedded grainstone-packstone lithofacies must have been deposited in a high-energy environment that was influenced by both marine and terrigenous input. The depositional lows into which it was deposited may have resulted from erosional channeling or by deposition in trough-shaped areas between constructional topography. For the southern example, the terrigenous material may represent material eroded from the Lane delta to the south, which perhaps was redeposited in depositional lows where tidal energy was focused. This interpretation of erosion of the Lane delta also is consistent with the absence of the middle Farley interval along the top of the delta. The example from the southwest (locality HM) is somewhat similar to the Pennsylvanian strata at Hamilton Quarry described by Feldman *et al.* (1990) in which a conglomerate was deposited in a system of relatively high-energy barriers and tidal inlets, mainly as part of an estuarine and lagoonal complex. In the Farley, the association of fossiliferous siltstones and cross-bedded facies suggest a similar setting to that of Hamilton Quarry. The example from the south (localities SRO, C5) is similar to that described by Cunningham and Franseen (1992) for a unit possibly equivalent to the Captain Creek Limestone. They suggested that such grainy units were

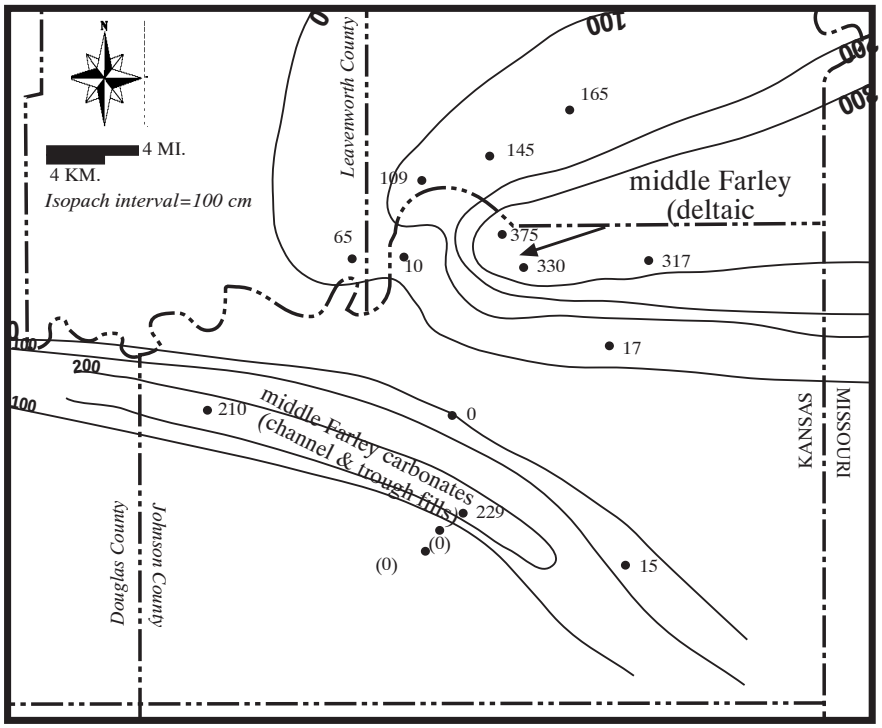

Figure 2.36. Isopach map showing thickness variations of the middle Farley Shale. The main delta lobe extends into the area from the northeast (arrow). The southern portion of the middle Farley is interpreted to represent a barrier bar and distributary channel system located off the distal end of the delta. Data from current study.

deposited in tidally influenced, topographic lows between algal build-ups where elevated energies resulted from constriction and focusing of tidal energies.

Local accumulations of skeletal wackestone-packstone also occur within the middle Farley at SRS and SRBS (Figures 2.30, 2.33, 2.34: Feature 18). At locality SRS, this facies is highly argillaceous and represents accumulation of argillaceous carbonate as a facies of the middle Farley. This argillaceous carbonate accumulated in what may have been a slight topographic low adjacent to the distal end of middle Farley deltaic deposition. The origin of the skeletal wackestone-packstone at SRBS is more problematic. This accumulation of skeletal wackestone-packstone is not argillaceous and contains only fine, fragmental skeletal material. It is also likely to be a facies of the middle Farley deltaic deposits but is less argillaceous due to a slightly more distal setting. The distribution of these facies are difficult to explain and with only two occurrences in the Farley no obvious control on their distribution is clear.

Isopach mapping for the middle Farley interval indicates that the underlying topography had an impact on the distribution of middle Farley deposits. Judging from the thicknesses, the deltaic siliciclastics of the middle Farley had a northeastern source (Fig. 2.36) and seem to have terminated against the thickened portions of the lower Farley (Figures 2.35 and 2.36).

Top of the Middle Farley-Upper Farley Interval

The lithofacies at the top of the middle Farley interval (Figs. 2.30 to 2.34: Feature 16) suggests that deposition of the upper Farley carbonates was initiated following a relative rise in sea level. This relative sea-level rise is indicated by the thin layer of fossiliferous siltstone that overlies the nonmarine blocky mudstones (Figures 2.30 to 2.33: top of Feature 16). This layer represents a marine flooding unit, and the base of this fossiliferous siltstone bed represents the fourth significant surface in the sequence

stratigraphic framework (Figure 2.30-2.34: Surface D). This siltstone lithofacies was deposited only in parts of the field area closest to the source of middle Farley siliciclastics.

The *Osagia* marker bed (Figs. 2.30 to 2.34: Feature 19) generally marks the next event of the flooding. This marker bed is found in most of the field area and is recognized by the presence of *Osagia*-brachiopod packstone near the base that grades up to phylloid-algal facies. This widespread consistency of facies indicates that there may have been little to no depositional topography that would have compartmentalized environments and lithofacies as occurred in the lower Farley interval.

There are, however, some places in which the marker bed is missing. One locality (C6) in the center of the field area, from which the distinct marker bed is absent and which contains no middle Farley siliciclastics, provides a potential correlation problem. A thin oolite bed (Fig. 2.30: Feature 20) is present, however, that is correlated with the marker bed. Evidence that this correlation is correct is found to the south at OAQ and the southwest at HM. The marker bed at both of these localities contains abundant ooids that were likely to have been transported from the accumulation of oolite located on a slight topographic high located in the center of the field area (C6). The marker bed is also missing towards the southeast (locality RQ), which is possibly due to deeper water caused by regional dip, which was not conducive to formation of the *Osagia*-brachiopod packstone facies.

The dominant facies of the upper Farley is the phylloid-algal facies, which is present in all localities except one (C4) (Figures 2.30-2.34: Feature 21). This facies is consistent in character throughout the area and shows only gradual thickness change (Figs. 2.30 to 2.34, 2.37) and less facies variation relative to the deposits of the lower and middle Farley. This relatively gradual thickness variation and lateral consistency in facies may be a result of subdued depositional topography. By this stage of Farley deposition,

most depositional topography had been reduced by filling with the deposits of the Lane-Island Creek as well as the lower and middle Farley. Therefore, the upper Farley exhibits much greater consistency in both thickness (Fig. 2.37) and lithofacies (Figures 2.30 to 2.34).

Localized accumulations of peloidal, skeletal packstone occur along the top of the upper Farley (Figures 2.30-2.34: Feature 22). This lithofacies indicates higher energy was present in some areas near the end of upper Farley deposition. Similar to occurrences of this facies in the lower Farley, the distribution of these peloidal, skeletal packstones in the upper Farley is somewhat enigmatic. Those located in the east (Figure 2.32: localities C3 & C4) are thin and located between areas of thickened phylloid-algal limestones. Here, even the *Osagia* marker bed is missing, suggesting erosion. It is possible that the peloidal, skeletal packstone was deposited in this area due to higher energy levels that resulted from concentration of currents between thickened accumulations of phylloid algal facies. This higher energy level then resulted in the erosion of some of the underlying facies, such as the *Osagia* marker bed, at C4.

At localities farther to the west (SRS and HM) the peloidal, skeletal packstone facies resembles the upper part of the Argentine Limestone, where it had been interpreted as a possible hardground. This is especially true at locality HM in the southwest, where there is an undulating but razor-sharp contact with the phylloid-algal facies below and where the peloidal facies also has a distinctly reddish color. The peloidal, skeletal packstone facies varies from approximately 20 to 100 cm in thickness in this locality. At locality SRS it is similar in appearance to that at HM but constitutes a single massive bed approximately 1.5 m thick along the top of the upper Farley. This bed is very even in thickness and flat-topped throughout the quarry and contains abundant, large bivalve fossils along the upper surface that suggest that this surface may have been encrusted with bivalves. These occurrences of peloidal, skeletal facies

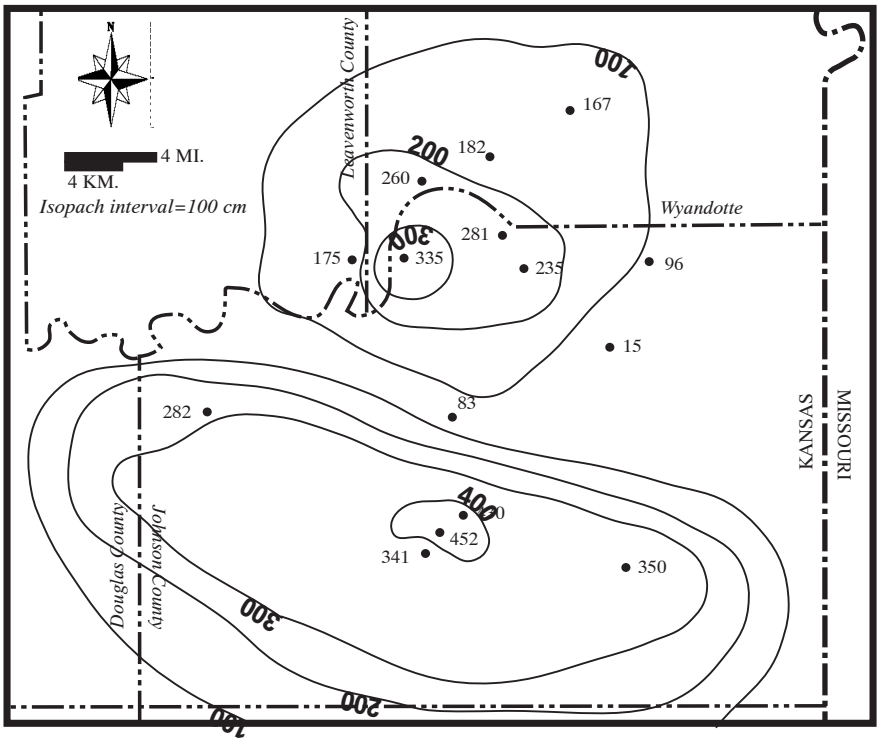

Figure 2.37. Isopach map showing thickness variation of upper Farley interval. The thickness variations of this interval are more gradual than those found in underlying units (Figs. 2.3, 2.4, 2.35, 2.36). This is likely due to subdued depositional topography that followed deposition of the Lane-Island Creek and the lower-middle Farley intervals. This subdued topography allowed for more even facies and thickness distribution in the upper Farley.

are likely to have been the result of the development of a hardground along the top of the upper Farley which is missing in surrounding localities due either to nondevelopment or to erosion prior to the deposition of the overlying Bonner Springs Shale. Evidence of Bonner Springs erosion is further discussed below.

Deposition of the Farley Limestone was terminated by the next influx of siliciclastics. The overlying Bonner Springs Shale is a thick sequence of marine and nonmarine siliciclastics that contains evidence of widespread subaerial exposure and erosion (Enos *et al.*, 1989; Watney *et al.*, 1989; Arvidson, 1990; this study). For example, at locality OAQ in the south (Fig. 2.30: Feature 23) the lower part of the Bonner Springs Shale comprises a coarse-grained conglomerate that contains large (centimeter scale) clasts of what appear to be upper Farley phylloid algal facies. Other evidence of erosion previous to deposition of the Bonner Springs Shale is found in the Hunt-Midwest Sunflower quarry (locality HM) to the southwest. In this quarry, the upper Farley could be seen to start to pinch out apparently from erosion prior to deposition of the overlying Bonner Springs Shale. For this reason, the final significant stratigraphic surface in the framework of the Farley Limestone (Figs. 2.30 to 2.34: Surface E) is drawn as a sequence boundary along the upper surface of the Farley Limestone.

Conclusions

The lateral and vertical variability observed in the Lane-Island Creek Shales and the Farley Limestone is the result of the interaction of fluctuating relative sea level, depositional topography, and the source direction and distribution of siliciclastics. Fluctuating relative sea level acted on a regional scale to cause large-scale changes in deposition such as the influx of deltaic siliciclastics or subaerial exposure of certain units.

On a more localized scale, depositional topography had the greatest control on the lateral and vertical distribution of lithofacies by influencing depositional environments.

The presence of two thick deltaic sequences overlying the marine Argentine Limestone indicates a relative fall in sea level between Argentine Limestone deposition and the deltaic Lane-Island Creek shales. Although delta lobe switching could explain the deltaic influxes, the presence of two separate deltas that entered the area from different directions during the same time would be unexpected with delta lobe switching. A lack of evidence of subaerial exposure in the Lane-Island Creek or along the top of the Argentine Limestone indicates that the fall was not extensive enough to expose the upper surface of the Argentine within the study area. The interpretation therefore, is that the upper surface of the Argentine represents the correlative conformity of an unconformity that was likely to have been located further to the north. The relative sea-level fall was, however, great enough to allow deltaic sediments to enter the area from both the north and south.

The lateral distribution of these deltaic sediments was closely controlled by the depositional topography of the underlying Argentine Limestone. The Island Creek deltaic deposits extended into the area from the north through a trough-shaped depositional low between two highs in the Argentine Limestone. In this manner, the Island Creek delta behaved as a valley fill rather than as a traditional delta lobe. The distribution of the southern Lane delta was also controlled by Argentine topography. The Lane shows a broader distribution due to fewer topographic restrictions in the Argentine Limestone to the south. In areas between the two deltas that received no influx of deltaic siliciclastics, a marine hardground developed along the upper surface of the Argentine Limestone.

The presence of a flooding unit and fully marine deposits along the top of the thickened Island Creek delta in the north indicates the termination of deltaic deposition in

the Island Creek delta. The change to carbonate deposition could have resulted from a relative rise in sea level or by a delta switch with no accompanying sea-level rise. The presence of a marine, carbonate-rich unit along the top of the Island Creek delta, however, indicates a relative rise in sea level.

Siliciclastic influxes remained somewhat active through lower Farley deposition, however, and its effects are represented by successions of alternating argillaceous phylloid-algal limestones and fossiliferous siltstones at several localities in the northwestern and central portions of the field area. As with the previous Island Creek siliciclastics, these pulses of deltaic siliciclastics were deposited in topographically low areas.

Following the relative sea-level rise, carbonate production was established throughout the northern and central area and depositional topography played a major role in the lateral and vertical distribution of lithofacies. High energy facies such as oolite and peloidal, skeletal packstone accumulated across topographic highs along the thickened Island Creek delta, whereas more quiet-water facies like phylloid algal boundstone and packstone and skeletal wackestone-packstone accumulated in the topographic lows where current energies were weaker.

Near the end of the lower Farley interval, higher energies were present, and as a result peloidal, skeletal packstones and oolitic, peloidal packstones accumulated along the top of the lower Farley in many places. These facies are found over and adjacent to some topographic prominences but are not found over the highest highs. Furthermore, there is evidence for subaerial exposure in the oolitic, peloidal packstones which are immediately overlain by additional marine facies. This relationship suggests that sea-level dropped then rose briefly before continuing to fall again. This could help account for the odd distribution of peloidal, skeletal packstones along the top of the lower Farley.

Lower Farley carbonate deposition was terminated by the influx of middle Farley siliciclastics into the area from the east-northeast. Like the deltaic influx of the Lane-Island Creek, the middle Farley delta influx followed a relative fall in sea level. This fall, however, was great enough to expose much of the delta in the study area and paleosols developed leading to the interpretation of a second sequence boundary. Associated with this deltaic influx was the deposition of the sandy, skeletal grainstone-packstone facies. This facies represents a high-energy environment located in tidally influenced channels or in trough-shaped topographic lows through which current energies were focused.

A second relative rise in sea level is indicated by a second marine flooding unit (fossiliferous siltstone) found along the top of the subaerially exposed middle Farley delta. This flooding unit is overlain by the fully marine upper Farley, which is relatively consistent in thickness and facies throughout the area. This consistency in facies is likely to be due to a relative lack in existing depositional topography. By this point in the deposition of the Farley Limestone, most depositional topography present starting with the Argentine Limestone had been filled with the deposits of the Lane-Island Creek shales as well as the lower and middle Farley limestones.

Finally, carbonate deposition of the Farley Limestone was terminated by a major relative sea-level fall that resulted in the accumulation of the Bonner Springs Shale and widespread exposure, erosion and paleosol development.

The complex distributions of carbonate and siliciclastic lithofacies described in the Lane-Island Creek and Farley Limestone illustrate the profound effect of paleotopography on the rock record. It was shown that carbonate and siliciclastic deposition responds to factors related to energy and accomodation, which in turn are greatly influenced by depositional topography. Siliciclastics are commonly focused into paleotopographic lows of

various origins; and, unlike what would be commonly expected, phylloid-algal facies of this interval seem to have a tendency to also fill lows rather than to accumulate on the highs.

Chapter 3: Geologic Factors Affecting the Quality of Limestone Construction Aggregate

Introduction

The goal of this study is to evaluate geologic and physical properties of limestone aggregates in an attempt to find criteria that can be used to quickly and efficiently identify highly durable aggregates and those subject to decay over time. Most past concrete aggregate-related research in Kansas has concentrated on a type of deterioration known as d-cracking. D-cracking is characterized by fine, closely spaced, parallel cracks that have blue, black, gray, or white deposits in the crack at the pavement surface. It typically develops parallel to joints or cracks in the pavement. (Crumpton *et al.*, 1994).

An early study related to d-cracking was conducted by the Kansas Department of Transportation (KDOT) in 1944 and suggested a significant relationship between coarse aggregates and d-cracking. As a result, the sizes of aggregate used in pavement concrete were reduced, resulting in improved pavement performance. In 1973 Bukovatz *et al.* presented the results of another study on d-cracking and again concluded that coarse aggregates and specifically coarse limestone aggregates were a main cause of d-cracking. They stated that pavements that contained more than 35 percent coarse limestone aggregates were more likely to be d-cracked than pavements with less than 35 percent coarse limestone aggregates. Most pavements without limestone coarse aggregate were rated as good.

Best (1974) reported the results of a seven-year study with the goal of finding a specific cause for d-cracking. Although this study concluded that the exact cause of d-cracking still remained a mystery, it was suggested that the freezing and thawing of water within the pavements was a main contributor. This study also supported the previous suggestion that coarse, limestone aggregates were a cause of the problem.

Based on the results of the early studies and those reported by Bukovatz and Crumpton (1981), KDOT adopted new requirements for selecting limestone aggregates. The plan adopted was to evaluate each quarry, subdivided into beds, and to approve or reject each individual bed based upon the results of laboratory freeze-thaw testing of concrete beams containing the coarse limestone aggregate from each bed (Wallace & Hamilton, 1982). Those aggregates that meet a minimum set of requirements concerning durability, freeze-thaw resistance and expansion are considered class 1 aggregates and are approved for use as construction grade material. The testing system outlined by the 1982 report is used today, and the use of aggregates meeting the established criteria has reduced occurrences of d-cracking. The tests are costly and time consuming, however, taking a minimum of six months to perform.

This paper reports attempts to identify geologic parameters that can be used to identify quality aggregates more easily. During the preliminary stages of the project several quarries currently producing class 1 limestone aggregate in eastern Kansas were visited. The units examined included the Tarkio Limestone, the Merriam and Spring Hill Limestones, the Argentine Limestone, and the Farley Limestone. Based on preliminary observations of outcrops and hand samples at the start of this study, specific geologic variables to be discussed seem to affect whether a unit passes or fails the class 1 aggregate physical tests. These variables allowed the development of several general working hypotheses testable in the Farley Limestone.

(1) Micrite-rich, phylloid-algal lithologies consistently produce durable aggregates.

(2) Fine-grained, matrix-rich limestones tend to pass, whereas coarser carbonate grainstones with coarse cements tend not to pass.

(3) High amounts of acid-insoluble residue in the rock has a negative impact.

(4) Distinct, sharp stylocumulates and shale beds have little or no impact on durability, whereas diffuse stylocumulates have a negative impact.

(5) Argillaceous limestones tend to fail testing; therefore the presence of clay minerals in the insoluble residues has a negative impact.

(6) Abundant, coarse, sparry calcites in the rock have a negative impact.

This study uses the Farley Limestone as a test case because it varies significantly both laterally and vertically in aggregate quality and allows initial testing of all of the hypotheses. If an understanding of how geologic factors interact to produce high-quality rock in the Farley is established, an analog for other similar limestone units in different locations can be developed.

Methodology

To gather data on the various geologic variables, detailed measured stratigraphic sections were described in eight quarries. Included in these sections were both active and inactive quarries from which KDOT has produced both class 1 and nonclass 1 aggregates from the Farley Limestone. All stratigraphic sections were measured at or near the locations from which KDOT had recently tested aggregates. Also included in the stratigraphic study were descriptions of outcrops and drill cores. These sections helped fill gaps between quarry exposures so that a more accurate stratigraphic reconstruction of the field area was possible. Information obtained includes bedding nature, preliminary lithologic classification, fossil types, and the percentage of the rock volume composed of sparry calcite. Descriptions of outcrops also emphasized determining the percentage of each stratigraphic interval that contained clay-rich zones. Shale beds, concentrated stylocumulates, diffuse stylocumulates, and disseminated argillaceous material were documented. Percentages of the total section that contained each form of argillaceous material were recorded. The different types of clay-rich zones are discussed in greater detail below. Measured stratigraphic sections are in Appendix 1.

After stratigraphic sections were measured and described in the field, samples were collected. For each of the stratigraphic sections, hand samples were collected, and polished slabs

and thin sections were made. These slabs and thin sections allowed a more accurate, detailed description of each lithology using the Dunham classification for carbonate rocks (Dunham, 1962). The descriptions include dominant depositional fabric, identification of fossils and other carbonate grains, and a more accurate estimation of the percentage of sparry calcite.

In addition to hand samples, 10 bulk rock samples of 250 pounds each were collected and turned over to the Materials and Research Division of KDOT for physical testing according to their established guidelines and procedures. After initial crushing of these ten samples, three pounds of the crushed aggregate was obtained from KDOT for each sample. This split included both $^{3}/_{8}$ inch and $^{1}/_{2}$ inch crushed aggregate. Independent tests conducted on the crushed aggregates included determining acid insoluble residue percentage, grain-size distributions of insoluble residues, x-ray identification of residues, and thin-section petrography to examine lithologies and spar content. Procedures for each of these tests are given in Appendix 2.

KDOT Physical Tests

Ten 250 pound rock samples were obtained from the Farley Limestone in Johnson and Wyandotte counties and were identified as sample numbers KU-1 to KU-10 (Appendix 1, Figures A1.2-A1.10). These samples were then tested by KDOT using the normal testing protocols prescribed by KDOT to determine aggregate durability. Physical test data for samples recently tested by KDOT from the Farley Limestone are also used in the study. These samples are referred to as KDOT-1 to KDOT-20, and stratigraphic locations of these samples are also indicated on the measured sections in Appendix 1. Stratigraphic sections were measured and described at or near the site of the KDOT sampling, so their test results could be compared directly to field observations.

The following sections summarize the parameters measured by the physical tests conducted by the Materials and Research Division of KDOT. The results of these tests constitute the data that are compared to data on geologic variables.

Absorption

Absorption is a measure of porosity and permeability of an aggregate sample and is determined as part of the physical tests conducted by KDOT. The reported value is given as a percentage of weight gain after soaking the aggregate in water for 24 hours. See Appendix 2 for procedures and calculations.

Modified Freeze-Thaw Test (Soundness)

The modified freeze-thaw test (soundness) is used as the first cut to determine whether an aggregate will undergo additional testing. The test determines an aggregate's resistance to freezing and thawing and is performed on raw aggregate that has been size graded and weighed. The aggregate is size graded so that only $^{1}/_{2}$ and $^{3}/_{8}$ inch aggregates are tested. Following 25 cycles of freezing and thawing, the aggregate is size graded again and reweighed to determine how much mass the original sample has lost . The reported freeze-thaw value is the percentage of the aggregate's original mass that is retained after 25 cycles of freezing and thawing. If the modified freeze-thaw value is 0.85, the value reported in this study would be 85 percent. This indicates the sample lost 15 percent of its mass due to degradation from freezing and thawing. At present, KDOT requires a minimum modified freeze-thaw value of 0.85 to continue with testing. If samples do not have a 0.85 modified freeze-thaw value, they are classified as nonclass 1, and no further tests are conducted on that aggregate. See Appendix 2 for procedures and calculations.

L.A. Wear Test

The L.A. wear test examines the resistance to degradation by abrasion and impact of the limestone aggregates using the ASTM Test C131-89. It is done by size grading the aggregates, weighing them, and tumbling them in a large rotating drum with several large steel balls. Following the test, the aggregate is resized and weighed again. The value reported indicates the percentage of the original mass lost due to size reduction from degradation by abrasion and impact. This test is not typically useful in classifying aggregates relative to durability.

Expansion

Expansion percentages are determined as part of ASTM Test C666-92 Procedure B. It is accomplished by making three concrete beams out of the limestone aggregate to be tested and a standard cement mix. Two pins are placed in the beams, and after the beam is cured a precise measurement of the distance between the pins is measured. The beam is subjected to cycles of freezing and thawing; at periodic intervals the beam is examined and the distance between the pins is remeasured. The value reported is a percentage of expansion over the original measurement. KDOT currently uses an average of 0.02 percent expansion for the three beams as the maximum expansion limit allowed for class 1 aggregate. See Appendix 2 for procedures and calculations.

Durability Factor

Durability factor is used to indicate an aggregate's durability and resistance to freezing and thawing. The durability factor is determined using ASTM Test C666-92 Procedure B. The value is related to the percent change in the fundamental transverse frequency of the beams, which is reported as the relative dynamic modulus of elasticity. The modulus of elasticity is a ratio of stress to strain in the elastic region and is an overall measurement of stiffness of a material. The durability factor measures the change in stiffness of the beams after a specified number of cycles

of freezing and thawing. Currently, KDOT requires a durability factor of at least 95 to qualify an aggregate as class 1. See Appendix 2 for procedures and calculations.

Lithologic Parameters

The following sections summarize the specifics of lithologic parameters that were compared to the results of the KDOT physical tests.

Lithology

Lithology was determined by examination of outcrops, hand samples and thin sections. Aspects of lithology considered include depositional fabric (Dunham textural classification), matrix type, fossils, and grain types. Comparing lithology to KDOT physical tests allows for identification of lithologies that might consistently produce durable aggregates. Lithologic examination also allows conclusions concerning the importance of micrite and microspar versus coarser cement (sparry calcite). Although these lithologic properties are qualitative in nature, there is potential for the identification of characteristics that are important in aggregate durability.

Spar Content

Accumulations of coarse spar (clear, crystalline calcite) constitute 10 to 60 percent of the limestones in the Farley. These spar accumulations resulted from either cementation of pore space or neomorphism of micrite matrix. In the Farley Limestone, sparry cement is found in fractures, in molds, and in original pore spaces between or within grains. Neomorphic spar fabrics are also common in the Farley Limestone and dominated by microspar and pseudospar fabrics with crystals defined by Folk (1965) to be in the range of 4 to 50 micrometers in size.

<u>Bulk Spar Percentage</u>

For the purpose of this paper, bulk spar percentage is defined as the percentage of the rock composed of visible, coarsely crystalline material including fracture fillings, spar-filled fossil molds, replaced fossils, and any spar-filled interparticle porosity (Figure 3.1). Estimates of spar content were made from examination of quarry outcrops and from cut and polished hand samples. Any visible accumulation of spar larger than approximately 0.5 mm was considered in the estimate. The value reported is an estimate of the total percentage of the rock volume that is composed of spar.

Average Spar Crystal Size and Crystal Form

By examining thin sections made from hand samples of each rock subjected to KDOT physical tests, average spar crystal size for each sample was determined. Because 80 to 90 percent of micrite matrix in the rocks of the Farley Limestone was recrystallized to microspar or pseudospar, those crystals finer than 50 micrometers are considered matrix and are not included in the estimates of average crystal size. Also noted during examination of thin sections were various types and shapes of spar present in the rocks. Table 3.1 is a summary of how the spar was classified and described.

Spar Percentage of Crushed Aggregates (Aggregate Spar)

As defined for this paper, spar percentage of crushed aggregates, referred to as aggregate spar, refers to the percentage of rock composed of spar following crushing and sorting of the original rock. This estimate includes only spar coarser than 50 micrometers. Any spar finer than 50 micrometers is considered matrix and therefore is